



Hydrodynamic Analysis of a Flopping NACA0012 Hydrofoil and Dolphin Fish-Like Model

T. Prabu[†], A. Firthouse and A. M. Baranitharan

PSG College of Technology, Coimbatore, Tamil Nadu, 641004, India

[†]Corresponding Author Email: tpr.mech@psgtech.ac.in

ABSTRACT

Imitating Dolphin fish-like movement is productive method for enhancing their hydrodynamic capabilities. This work aims to analyze and understand the oscillations of tail fluke of Dolphin, which can be used as a propulsive mechanism for underwater fish robots and vehicles. The objective of the work is to achieve the desired oscillating amplitude by simulating the NACA 0012 profile using computational models and Set up the swimming movement of the dolphin, imitating a fish like model. Computational techniques were employed to examine the propulsive capabilities of the oscillating hydrofoil, inspired by the dolphin's biological propulsion. The evolutionary of fluid pattern in the field surrounding both Dolphin fish model and the NACA0012 hydrofoil, from initial motion to cruising, was established, and the hydrodynamic impact was subsequently studied. An user-defined function (UDF) was developed to create a dynamic mesh interface with CFD code ANSYS FLUENT for establishing the oscillations of Dolphin tail across the flow field. Influencing hydrodynamic coefficients such as lift and drag coefficients at different frequencies were also obtained. The findings shown that when the acceleration of the Dolphin fish model increases, the time averaged drag force coefficient drops because The wake field's vortex disperses to have some beneficial effects and pressure of water surrounding the fish head intensifies to produce a large resistance force. Simulation results show a 98% agreement at lower frequency and speed levels but a 5% deviation at higher frequency and speed due to turbulence effects in both models. It was established that the vortex superposition enhances the Dolphin fish like model rather than lowering its positive impacts. The Strouhal number, which is obtained by the fluid field's evolution rule, can be linked to the Kármán vortex street span with reverse.

Article History

Received July 12, 2023

Revised October 30, 2023

Accepted November 17, 2023

Available online January 30, 2024

Keywords:

Dolphin, Fish-like Model

NACA 0021

Computational Fluid Dynamics (CFD)

Hydrodynamic Performance

Vortex Distribution

1. INTRODUCTION

Autonomous underwater vehicles (AUVs) represent a class of intelligent robots capable of independent movement without direct human intervention. These versatile, biomimetic machines can serve diverse purposes, including the detection of nuclear wastes, aiding in underwater search and rescue operations during emergencies, providing early warnings for tsunamis, identifying leaks in underwater pipelines, assessing water quality, sampling oceanic environments, and conducting centimeter-scale inspections of pipelines.

Biomimetic robot designs are established by translating biological principles into engineered systems. Researchers often draw inspiration from various

underwater creatures, mimicking their body forms and swimming capabilities in the development of these vehicles. Among the various aquatic animals, dolphins have garnered considerable interest due to their unique characteristics. The impressive movement of the Dolphin fish and its capacity to swiftly navigate through narrow areas serve as a source of inspiration for engineers looking to enhance the design of current AUVs. The Dolphin fish's propulsion is a result of the undulating movement of its tail. This type of movement is found to be quieter, more maneuverable, and efficient compared to the traditional propeller-based design (Guo et al., 2015; Chen et al., 2016).

Small underwater vehicles face limitations in efficiency, capped at 40% as pointed out by Triantafyllou

et al. (2000), owing to the generation of vortices perpendicular to their direction of travel. These vortices, due to their alignment, fail to generate thrust even at increased power consumption. Alternatively, an oscillating foil can be employed to generate thrust, utilizing the reversible Karman Vortex Street formation in the wake of the flowing water. The dependence of thrust creation on the Strouhal number bears a resemblance to the efficient propulsion exhibited by fish.

The use of the oscillating foil for propulsion is attributed to its superior energy conversion efficiency and its quieter operation in contrast to conventional motors. The bigger mammals like Dolphin fish propel itself by oscillating its Tail fluke. Several drag reducing mechanism of Dolphin tail was proposed, but nothing can able to solve Grey's Paradox. The dolphin propels itself by oscillating its tail. When the tail oscillates in the water, the tail pushes the water down and the water will in turn push the tail back, hence the thrust force is generated. It is the reason why the dolphin can able to reach high swimming speed in highly dense and viscous environment. The Dolphin has a peculiar oscillation of its Tail Fluke when compared with other fishes, it has two degrees of freedom one is the translation along the Vertical axis and at the same time the Tail will have rotation about the axis perpendicular to the plane of view. Lauder (2011) states that fish are commonly perceived as highly proficient swimmers. Biologists and engineers have invested substantial effort in assessing the thrust efficiency of both swimming robots and living fish. The primary objective of these endeavors is to identify design and kinetic control principles that can be applied to create robotic fish capable of achieving exceptionally efficient propulsion. Streffling et al. (2011) developed an innovative submersible named the Synergistically Propelled Ichthyoid (SPI), which merges jet behavior with oscillatory movement using a undulating backend for propulsion. Simulations demonstrated the advantage of a fluttering tail over a rigid one and reveal the SPI's maneuverability with variable fluid velocity.

Triantafyllou et al. (2000) contributed significantly to the study of robotic fish by demonstrating the hydrodynamics of fish-like swimming through both Computational and Experimental fluid dynamics techniques. Jindong Liu and Huosheng (2004) investigated a three dimensional kinematics simulator for studying the hydrodynamic characteristics of a robotics fish. Their research demonstrated that the simulator offers a dependable forecast of the navigational behavior of a robotics fish. Leroyer and Visonneau (2005) dealt with 3D mathematical models calculation on a own propelled body resembling a fish based on Reynolds-Averaged Navier-Stokes (NS) Equations. They anticipated how the body's shape would deform and how it would interact with the fluid forces, impacting its movement. Gen-Jin Dong and Xi-Yun Lu (2005) investigated the behavior of fluid motion of a fish movement subjected to certain streamwise traveling waves using a wave plate which imitates the oscillation of a fish backbone motion during swimming action. Mohammadshahi et al. (2008) studied the forces exerted by fluids in motion on objects within them of a fish like

swimming bionic mechanical device through CFD modeling, compared the results with fabricated physical models. In the earlier study of, Borazjani et al. (2012), conducted an analysis of the fluid dynamics involved in the C-start maneuver of a bluegill sunfish through three dimensional numerical simulations.

Wen et al. (2013) discovered the arrangement, structure of swirls in the circulation produced along fish couldn't a straightforward mirror image of the Kármán vortex street. They constructed an artificial fish model and conducted a comprehensive fluid dynamic behavior. Zhou et al. (2015) They put forth a computational model for investigating the hydrodynamics of bio-inspired fish swimming, employing a CFD (Computational Fluid Dynamics) model, and devised a filtering algorithm to integrate near-body pressure into the external flow field. The researches of Wu et al. (2015) demonstrated that velocity and force display noticeable fluctuations during self-propelled swimming. Ren et al. (2015), Wang et al. (2015) developed a robotic dolphin with an operation of voluntary movement through artificial intelligence. Li et al. (2017) developed a numerical system based on procedure of 2D NS to solve realistic biological problems. Zhang et al. (2018) studied the impact of kinematic models on fluid dynamic behavior in a self-propelled swimming channel and analysed thrust force generation mechanism.

Xue et al. (2020) developed a kinematic model to replicate fish swimming motions, allowing for modifications in the starting stage with peak fluctuating amplitude. They analyzed the hydrodynamic impact on the fish model, considering various densities, initial stages to sailing.

Ou et al. (2020) investigated the fluid dynamic behavior of a fish like foil oscillating very close to the vertical sidewall. They have used boundary-lattice Boltzmann method for verifying the impact of the Strouhal number (St) which is 0.1 to 0.5, and wavelength (λ) within the range of 0.6 times the length (L) up to 1.4 times the length (L) on the its characteristics and power utilized efficiency. These results indicated that as the Strouhal number (St) and wavelength (λ) increase, the wall forces also increase. However, the impact on power extraction efficiency is contradictory.

To achieve more precise performance predictions, it is essential for robotic dolphins to undergo hydrodynamic analysis during motion, particularly the repetitive motion, utilizing the Computational Fluid Dynamics (CFD) approach. CFD simulations, recognized as crucial tools for fluid analysis, have been extensively utilized to comprehend various intricate physical phenomena.

These studies have significant implications in unraveling the swimming mechanism of fish and aiding the advancement of submerged vehicles. Although, additional studies necessary for elucidate the fish's float technique and enhance the fluid dynamic performance of submerged vehicles. While the research mostly focus on stable cruising swimming, the initial propulsion process holds equal importance. The fluid dynamic impact of

Dolphin fish does not having sufficient evolution and rules are not explored.

The aim of this paper is to introduce a novel hydrodynamic analysis for a mechanical dolphin model that combines features of both traditional robotics and gliding mechanisms, often mimicking the movements and characteristics of real dolphins and its similarity with NACA0012 hydrofoil. Insights near-dolphin-body flow field is importance to enable submerged locomotion controllers with more efficiency and adaptability inside unknown surroundings. Taking inspiration from the way natural dolphins sense the flow field around their bodies, this research is conducted. A dolphin-like fish CAD model is developed and its flow and swimming characteristics is compared with NACA0012 hydrofoil. The motion behavior blueprint of the robotic dolphins is incorporated within the body and/or caudal fin, distinguishing it from a multitude of propulsion methods observed in robotic fishes. It is understood from the past researches that more attention is paid to the behavior of robotic fishes. The limited research works are available on swimming pattern of robotic dolphins and its similarity with NACA0012 hydrofoil. So, we have focused on directed towards acquiring more precise hydrodynamic characteristics of a gliding robotic dolphin and NACA0012 hydrofoil. The agreement between both the models is reasonable, future researches can be completed in shorter computational time and cost by using NACA0012 hydrofoil.

2. MODEL DESCRIPTION

As the cross section of Dolphin body and tail is geometrically similar to the available NACA0012 aerofoil, the usage of NACA0012 hydrofoil was verified with determination of hydrodynamic coefficients. This hydrofoil was modeled as a rigid body to avoid the complications of deformation of the hydrofoil under the static and dynamic loads, the focus was given mostly on its interaction with the surrounding fluid in the computational domain. Fig. 1 describe the general depiction of dolphin fish anatomy and NACA0012 hydrofoil profile.

The oscillation of the tail fluke of the Dolphin can be described in the Fig. 2. The first degree of freedom of the hydrofoil is the Pitching motion along Y-direction (can be along positive and negative Y-direction). The maximum translation along the Y-direction is the amplitude of oscillation of the fluke, denoted by A.

The other degree of freedom is the rotation about an axis perpendicular to the plane of view which is represented by the letter B in this picture. The translation along the Y-direction is called “plunging” of hydrofoil and the rotation about the axis perpendicular to the plane of view is called pitching motion. The unsteady forces to study the unsteady forces which are developed using the pitching and the plunging motion of the tail fluke is analysed in this work. Fig.3 displays the swimming process of both Dolphin like fish and NACA0012 hydrofoil.

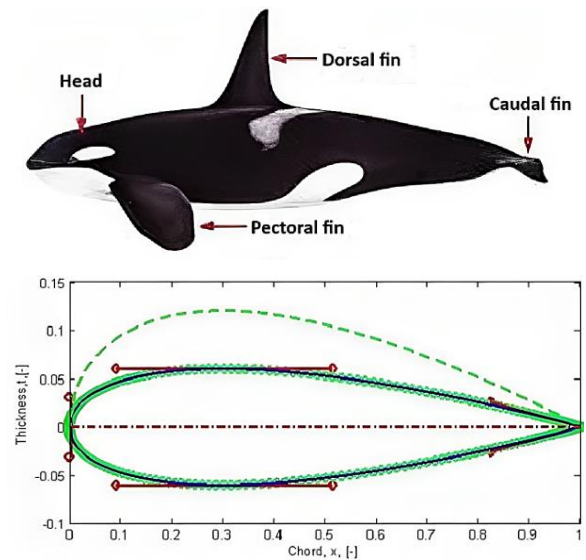


Fig. 1 The general depiction of (a) Dolphin fish anatomy (b) Profile of NACA0012 hydrofoil

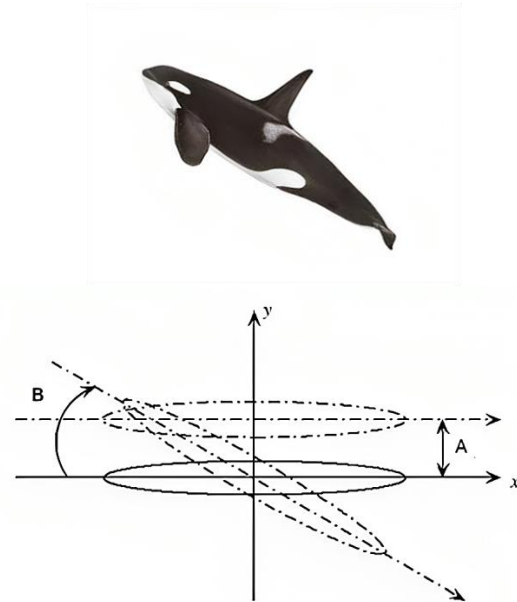


Fig. 2 Pitching and Plunging motion of Dolphin Tail

Table 1 explains the parametric dimensions of dolphin fish model and Table 2 shows the parametric dimensions of NACA0012 hydrofoil model with description as follows

Maximum Thickness (0.12@30% C): The NACA0012 hydrofoil has its maximum thickness, which is 12% of its chord length (C), occurring at 30% of the chord length from the leading edge.

Maximum Camber (0 @100% C): it maintains the same shape along its entire chord length.

Trailing Edge Gap (0% C): The hydrofoil has a sharp trailing edge with no gap, providing a clean and continuous rear edge.

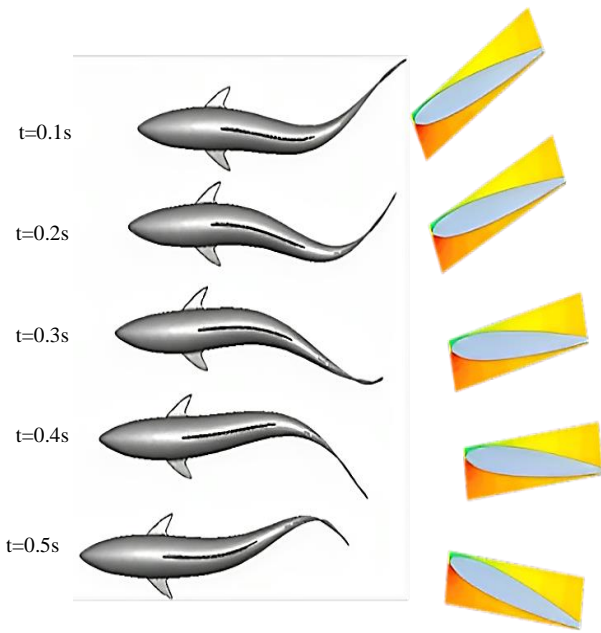


Fig. 3 swimming process of both Dolphin like fish and NACA0012 hydrofoil

Table 1 Parametric dimensions of Dolphin fish-like model

| Parameter | Value |
|------------------------------------|-------|
| Nose to tail length, L [m] | 2.5 |
| Volume [m ³] | 0.152 |
| Peak-to-peak tail amplitude, A [m] | 0.148 |
| Depth from free surface [m] | 1 |

Table 2 Parametric dimensions of NACA0012 hydrofoil

| Parameter | Value |
|-------------------|------------|
| Maximum thickness | 0.12@30% C |
| Maximum Camber | 0 @100% C |
| Trailing Edge Gap | 0% C |
| Upper nose radius | 1.5% C |
| Lower nose radius | 1.5% C |
| Boat- tail angle | 16.32 Deg |
| Release angle | 0 |

Upper Nose Radius (1.5% C): The upper surface of the hydrofoil features a rounded nose with a radius of 1.5% of its chord length.

Lower Nose Radius (1.5% C): Similarly, the lower surface of the hydrofoil also has a rounded nose with a radius of 1.5% of its chord length.

Boat-Tail Angle (16.32 Deg): The hydrofoil tapers towards the trailing edge with a boat-tail angle of 16.32 degrees, potentially reducing drag and promoting streamlined flow.

Release Angle (0): There is no specified release angle for this hydrofoil, indicating that it doesn't have a specific angle at which it's designed to separate from the flow.

3. COMPUTATIONAL MODELING

In this research, a dynamic solution to the NS equations has been developed to analyze the viscous flow around the undulating Dolphin fish. Unsteady solutions to the incompressible NS equations are essential in comprehending highly unsteady fluid phenomena. The non-dimensional NS equations, represented in the x, y momentum conservative with mass are converted into a common coordinate system of curvilinear. This transformation allows for the equations to be expressed in an integral form, as demonstrated in Eq. (1).

$$\frac{\partial}{\partial \tau} \int_{S(t)} q dS + \oint_{1(t)} [(F + F_v)n_x + (G + G_v)n_y - qV_g n] dl = 0 \quad (1)$$

where,

$$q = \begin{bmatrix} u \\ v \\ p \end{bmatrix} \quad F = \begin{bmatrix} u^2 + p \\ uv \\ \beta u \end{bmatrix} \quad G = \begin{bmatrix} vu \\ v^2 + p \\ \beta v \end{bmatrix}$$

$$F_x = -1/Re \begin{bmatrix} 2u_x \\ u_y + v_x \\ 0 \end{bmatrix} \quad G_v = -1/Re \begin{bmatrix} u_y + v_x \\ 2v_y \\ 0 \end{bmatrix}$$

The continuity equation for mass conservation is modified by the introduction of an artificially incorporated time derivative of pressure. The velocity components of “u” and “v” to represent the vector “q” and pressure “p” are introduced. Meanwhile, S(t) is the cell of area which denoted as i & j. The motion of swimming Dolphin fish object was deformed continually, a body-fitted mesh method was introduced. This mesh generates and regenerates with respect to time. As a result, the grid velocity V_g is important for the governing equations.

To discretize the computation domain into small control volumes, the finite volume method is used. Time derivative was executed by Euler implicit scheme based implicit factorization approximate method. The applied foemula for this scenario was a first-order, 2 point backward-difference. Sub-iterations were created to satisfy the equation of continuity at each physical time step, taking into account the artificial compressibility relationship. A second order-upwind differencing method was used for the convective term. Gauss integration of finite volume method was employed for the viscous term.

3.1 Modeling of Dolphin Fish-Like Structure

For modeling of an undulating movement of Dolphin fish, adjustable stretching, rigid rotation, and the translation are the three basic motions of a moving body. In fixed coordinate system the translate movement is substituted by explicitly incorporating opposite forces into equation of momentum. This is more difficult for rotating and deforming motions. As a result, a moving mesh system is presented. To compute this unstable flow of swimming pattern of Dolphin fish, a regenerating grid procedure is fits for each and every time step of motion while keeping fixed outer atmosphere is required. Figure 4 shows the hydrodynamics forces and moments acting on the Dolphin fish body of transverse movements.

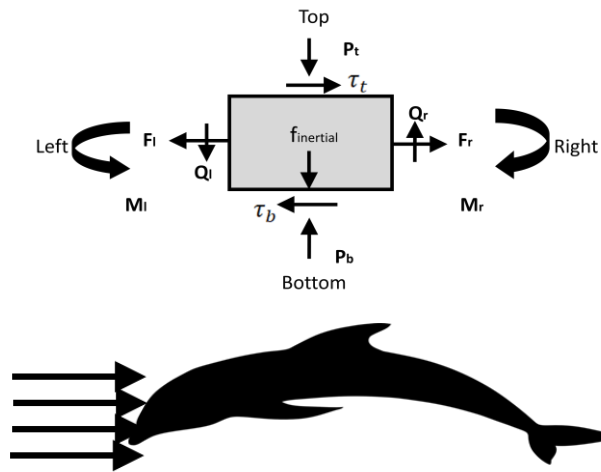


Fig. 4 Hydrodynamics forces and moments acting on the Dolphin fish body of transverse movements

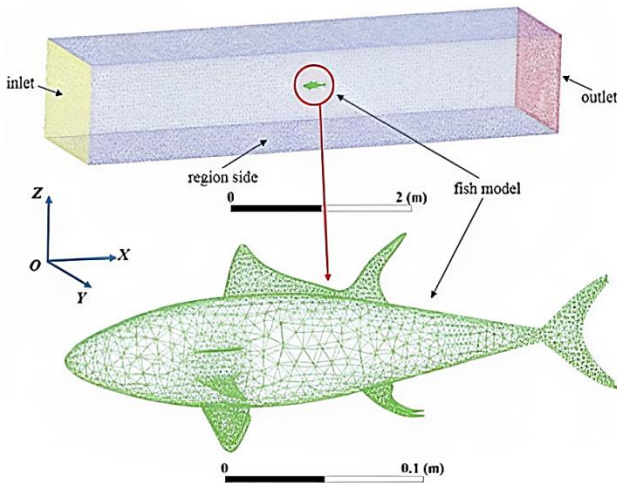


Fig. 5 Computational domain of Dolphin fish-like model

Borzjani and Sotiropoulos (2008) investigate the averaged the instantaneous values across multiple undulatory cycles of the robotic fish. To maintain the proportional relationship between power and thrust force in line with previous research, we standardized the characteristics as follows. Eq. (2a, 2b & 2c) refers the hydrodynamic coefficients of non dimensional coefficient used to measure the Dolphin’s performance while swimming are:

$$C_t = \frac{F_t}{0.5U^2 S_{body}} \quad (2a)$$

$$C_d = \frac{F_d}{2\rho U^2 S_{body}} \quad (2b)$$

$$C_l = \frac{F_l}{2\rho U^2 S_{body}} \quad (2c)$$

During undulatory locomotion, when combined across the entire body surface, the forces acting on segment substantiate individual. Because the bending moment is ignored due to the negligible value of angular rotation, simply regards related to fluid dynamics and momentum forces remains. To model the swimming



Fig. 6 Computation domain of NACA0012 hydrofoil

pattern of Dolphin, a sinusoidal function was created to describe a side wave that travels down the Dolphin towards the back tail end.

The wave has shape of (Eq.3)

$$Y_1(x, t) = a_1(x) \sin \left[2\pi \left(\frac{x}{\lambda} - \frac{t}{T} \right) \right] \quad (3)$$

The equations derived from Navier-Stokes are capable of providing the both large and small insights into the fluid area. The pattern can be described and visualized grid points or cell-centers. The pressure distribution and lateral stress acting on body of the deforming fish-like body are used to calculate thrust and lift. The following assumptions were made to capture these values: (1) Model is elastic body with constant length while travelling of swimming process; (2) waves are simply in sideways compressible movement. This table also includes the resulting peak-to-peak tail motion magnitudes. The dolphin fish-like model and the NACA0012 hydrofoil were simulated at depths of 2 m. Fig. 5 shows computational domain of Dolphin fish-like model.

3.2 Modeling of NACA0012 Hydrofoil

To mimic the movement of Dolphin fish tail, a similar shaped hydrofoil NACA0012 was considered for the analysis (Fig. 6). This was modeled using the CAD software SolidWorks as a 2D surface. Then, the surface was created using the profile and the part is saved as IGES file for exporting into the CFD code. In this work, an underwater hydrofoil is developed to characterize the efficient oscillating foil propulsion mechanism power and the ability to traverse in rectilinear and curvilinear paths. The Camber length of the hydrofoil is as 1 meter. Fig.6 shows computational domain of NACA0012 hydrofoil.

3.3 Domain Discretization and Grid Independence Study

The computational domain was developed by using a mesh count of 664, 807. This count was chosen after conducting a mesh independence study as shown in the Fig. 7. The Drag coefficient value reached the steady state, when the mesh count reached 664,807.

The details of domain discretization are given in the Table 3. The quality criteria explain in Table 4. Accordingly, this was considered as an appropriate mesh count to precede the simulation in the CFD code ANSYS 14.0 FLUENT.

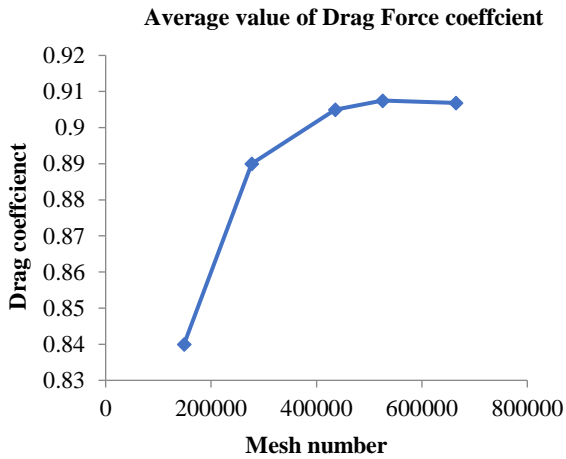


Fig. 7 Mesh Independence study

Table 3 Details of domain discretization

| Parameter | Value |
|------------------------------------|--------------------------|
| X-coordinate in meters | -4.0 to +4.0 |
| Y-coordinate in meters | -2.0 to +2.0 |
| Minimum volume in cubic meters | 6.67 x 10 ⁻⁷ |
| Maximum Volume in cubic meters | 1.091 x 10 ⁻⁴ |
| Minimum Face area in square meters | 4.85 x 10 ⁻⁴ |
| Maximum Face area in square meters | 1.42 x 10 ⁻² |
| Number of Nodes | 6, 62, 592 |
| Number of Elements | 6, 64, 807 |

Table 4 Mesh quality criteria

| Parameter | Quality criteria |
|---------------------|------------------|
| Cell angle | > 18° |
| Cell expansion rate | < 10 |
| Cell Skewness | 0.8 to 0.95 |
| Aspect Ratio | < 1000 |
| Orthogonal quality | > 0.6 |

The oscillations of the tail fluke are given to the hydrofoil by creating an add-on User defined function (UDF) which is the C-programme which governs the movement of oscillation. The pitching amplitude of oscillations provided in this analysis is 0.5m. The plunging amplitude is 0.5 rad. As the CFD code FLUENT didn't have its own compiler, a Visual Studios 2017 Community version based compiler environment was built to set the environment variables. When the hydrofoil oscillates inside the fluid domain, the mesh associated with the hydrofoil responds accordingly. To capture this, meshing technique called "dynamic mesh" was invoked, and the suitable numerical parameters were set to avoid the occurrence of error. This dynamic mesh zone is created by hooking the compiled UDF.

```
#include "udf.h"
#include "math.h"
```

```
DEFINE_CG_MOTION (shm, dt, cg_vel, cg_omega,
time, dtime)
{real omega; if (time<=1) {cg_omega[2]=-0.5;
cg_vel[1]=-0.5; }
else
{cg_omega[2]= +0.5; cg_vel[1]=+0.5; }
if (time>=3)
{cg_omega[2]=-0.5; cg_vel[1]=-0.5; }}
```

The realizable k-epsilon turbulence model pertains to a model. It was used to capture the physics of oscillating hydrofoil. The vortex street will be formed when the hydrofoil oscillates in the fluid. Hence the model should be able to capture the Vortex shedding from the hydrofoil. Furthermore, this model satisfies certain computational limitations on Reynolds stresses as well as conforms in turbulent flow physical rules. It can also simulate the impact of fluid a rotation on the turbulent stresses of boundaries liberated the shear moves and rotating uniform the shear travels in the fluid field surrounding the Dolphin fishlike model.

The number of time step and time step size was set as 385 and 0.01 seconds respectively to achieve desired oscillation of hydrofoil. Even though it was proven to use T/200 Li et al. (2017), in this work, T divided by 500 was set to time step size, resulting in a fluctuation period of T=1/f, where f is the Dolphin fish like model's undulating frequency. This time step will be expected to provide better accuracy. Governing equations were solved using SIMPLE algorithm and the second order upwind scheme for momentum equation and the first order upwind scheme for Turbulent Kinetic Energy and the Kinetic Energy Dissipation rate. The solution monitor is set to plot the Drag and the Lift forces developed against the time. A dynamic dolphin-like swimming simulation is realized through an innovative dynamic mesh and user-defined function (UDF). Furthermore, the corresponding turbulent simulation and SIMPLE technique compatible with dolphin like floating are carefully chosen for high accuracy and quality. The area that formed the limit was defined as the boundary condition, with wall velocity is zero in Dirichlet boundary, and input as a Neumann boundary condition, with change in velocity also zero, the outlet is same explains in Table 5. However, 0.01m/s as inflow velocity, approximately speed of cruising is 1%.

3.4. Validation of Numerical model

An experimental data of Anderson et al. (1998) was used to validate the present numerical model. He developed an experimental apparatus with a NACA0012 hydrofoil and conducted a series of experiments of

Table 5 Boundary Conditions

| Name | Boundary Type | Condition |
|--------|-------------------|-----------------------|
| Inlet | Velocity inlet | Re = 100-800 |
| Outlet | Pressure outlet | Gauge Pressure= 0 Pa. |
| Wall | No-slip condition | Zero velocity |

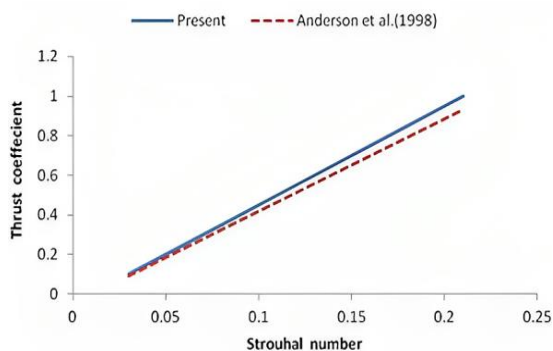


Fig. 8 Comparison of thrust coefficient between present work and Anderson et al. (1998)

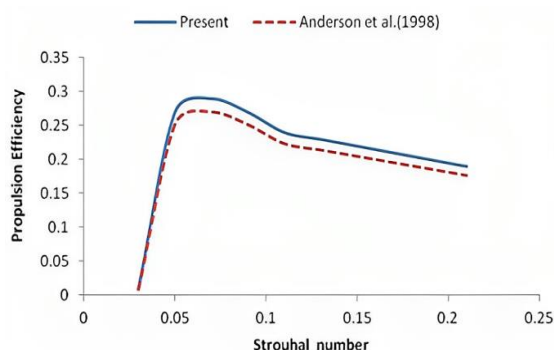


Fig. 9 Comparison of Propulsion efficiency between present work and Anderson et al. (1998)

various oscillation conditions. As shown in Fig. 6, a NACA0012 hydrofoil simulation model has been created and the fluctuating variables for heave amplitude-to-chord ratio $h_0/c = 0.25$, phase angle $\psi = 90^\circ$, and maximum angle of attack $\alpha_{max} = 15^\circ$ are chosen for evaluation. Parameters like standard thrust coefficient and propulsion efficiency are defined consistently across two works. The average thrust coefficient and propulsion efficiency calculated are measured and found reasonable agreement with the experimental data proposed by Anderson et al. (1998) as shown Fig. 8 and 9.

5. RESULTS AND DISCUSSION

5.1 Effect of Hydrodynamic Coefficients

In the first instance, the Dolphin fish model entered the speed motion to simulate self-propelled swimming. Opposite force was currently greater than the thrust force. The opposite force acting in the fish model which is called resistance force. When the speed increases, so does the resistance force also increase. Once both these forces achieved an equilibrium state, the Dolphin model entered into sailing. The Drag and Lift coefficients of self-propelled swimming are shown in Fig. 10 and Fig. 11 respectively.

The drag coefficient, symbolizing the amalgamated impact of thrust and resistance forces, varied in accordance motion of fluctuation in the Dolphin fish model. Over the course of the acceleration process, the

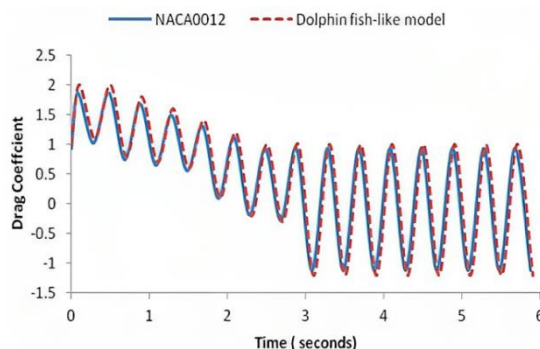


Fig. 10 Correlation of Drag coefficients of NACA0012 and Dolphin fish-like model

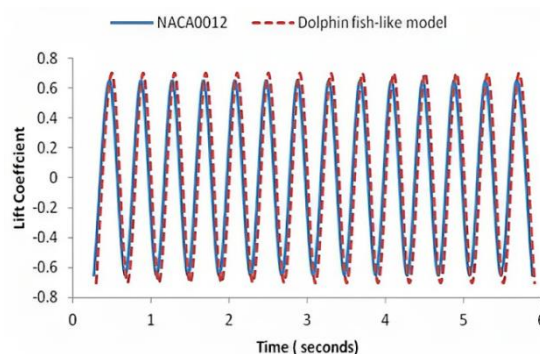
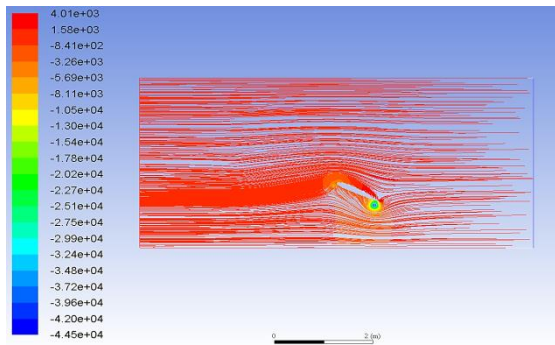


Fig. 11 Correlation of Lift coefficients of NACA0012 and Dolphin fish-like model

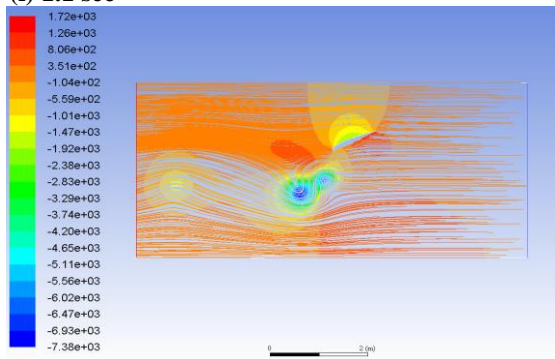
mean value of the drag coefficient diminished, leading the Dolphin fish model to transition sailing phase precisely on 2 seconds. Subsequent to this point, the drag coefficient oscillated around 0, here the velocity of front end is stable. Coefficient of the lateral forces approximately 0, mean value remaining constant at 0 throughout entire swimming procedure. It shown in Fig. 10 and Fig.11 that results of the both NACA0012 and Dolphin fish model provides good consistency. Despite some variation close to the highest point in the hydrodynamic coefficient curve, the overall trends are similar.

Vortex distribution is a vital parameter that affects the propulsive performance and also pressure variation is a dominant factor for propelling the fish model and NACA0012 model to move forward. As shown in Fig. 12(a), the founded moment of four pressure cloud picture were chosen and a vortex circulation. Moments A, B, C, D denote t_A, t_B, t_C, t_D are 0.47 s, 1.18 s, 1.96 s, and 2.59 s, respectively.

A pressure area showed up back the Dolphin fish like model and the NACA0012 models at time = 0.47 s. However, pressure plot disappeared in starting side. The variation of pressure between the area near to head and tail led to a comparatively higher coefficient of drag force value. The magnitude of the pressure is subsequently increased and expanded towards the model's frontal area. Distribution of pressure at leading & tail side was comparatively greater, as shown in Fig. 12(b). Simultaneously, the pressure a value decreased

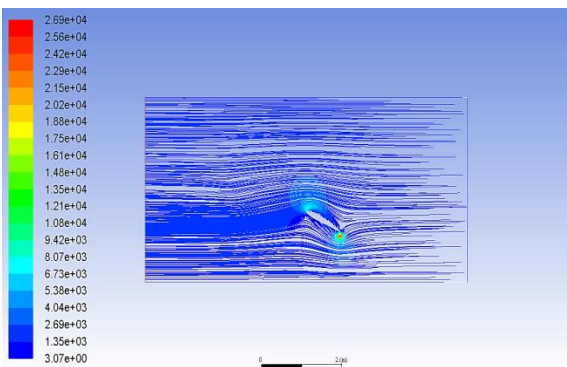


(i) 1.1 sec

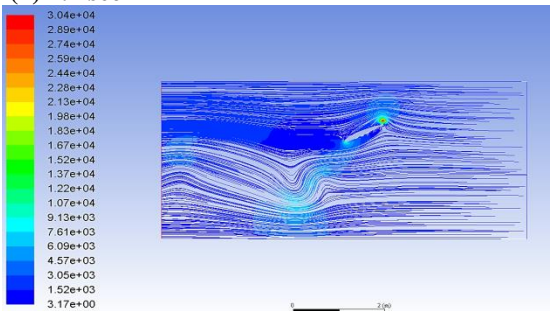


(ii) 3.1 sec

(a)



(i) 1.1 sec



(ii) 3.1 sec

(b)

Fig. 12 (a) Path lines colored by static pressure (b) Path lines colored by dynamic pressure

near the model's midsection. The generation of large resistance force would be possible if the oscillating magnitude of the front end was larger.

5.2 Effect of Reynolds Number on Vortex Distribution

Difference in pressure is the main driving force behind the Dolphin fish model and NACA hydrofoil to move forward. However, vortex is another vital

parameter that affects the propulsive performance. Fig. 12(a) and (b) show the pressure gradient nephogram associated with the Dolphin fish model and NACA0012 from the beginning to the end of the sailing process.

At $t=1.1$ seconds, the static pressure on the top surface of the hydrofoil is higher when compared with the bottom surface of the hydrofoil. This pressure distribution is responsible for the generation of thrust at $t=1.1$ seconds. At $t=3.1$ seconds, the static pressure on the bottom of the hydrofoil is higher when compared with the static pressure on the top of the hydrofoil. This is responsible for the generation of thrust at $t=3.1$ seconds.

At $t=1.1$ seconds the dynamic pressure is also high on the upper side of the hydrofoil when compared with the lower side. Similarly, at $t=3.1$ seconds the dynamic pressure in the lower side of the hydrofoil is high when compared to the upper side, and hence at $t=1.1$ and 3.1 seconds the total pressure on the upper and lower sides of the hydrofoil are high which is responsible for the creation of thrust and the lift at 1.1 and 3.1 seconds respectively.

5.3 Effect of Strouhal Number On Vortex Distribution

The Strouhal Number is a dimensionless factor to analyze unsteady, oscillating fluid flow dynamics applications. It is vital when analyzing unsteady nature of vortex separation frequency of Dolphin fish-like underwater vehicles. The Strouhal Number is a measure of the regional acceleration due to forces of gravity caused by fluctuations in the velocity of Dolphin movement from a single location in the flow field to another. The Strouhal Number can be expressed as Eq.(4),

$$S_t A = \frac{\omega l}{v} \tag{4}$$

As the Dolphin fish tail fluctuates in the swimming motion, the distinctive length always varies. This makes it difficult to ensure the certainty of the temporal value. In this context, computational fluid dynamics (CFD) can serve as an effective tool for assessing the Strouhal number by capturing the distribution of vortices. The Strouhal number is associated with reversed Kármán vortex street band (Wang et al., 2018; Hemmati et al., 2019).

Figure 13 demonstrates the relationship between Strouhal number (S_t) or non-dimensional oscillation frequency and Reynolds number. Starting from the unstable base flow at $Re=100$, oscillations were developed. As a result, the mean value changed and frequency increased accordingly. As the flow evolves from the base flow, Reynolds stresses kept grown. At later stage, the flow evolved to a point of marginal stability of the mean flow. The oscillatory frequencies measured at this point are the corresponding nonlinear Strouhal number.

Above $Re= 300$, the flow is time periodic. The Benard-von-Kaman vortex street and Vortex shedding occurred. The high thrust created in wake field in the

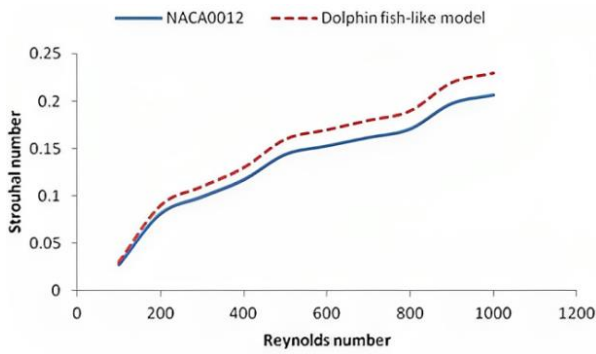


Fig. 13 Relation between Reynolds number and Strouhal number

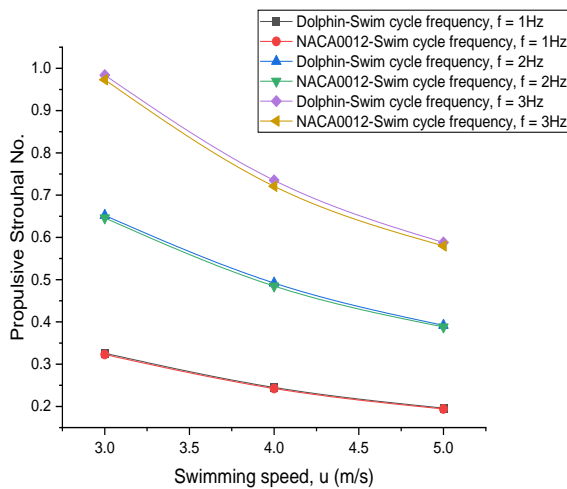


Fig. 14 Simulation results of Strouhal number

reversed Kármán vortex street. Brücker and Bleckmann (2007), However, both the cause and impact of vortex circulation remain unknown. The vortex existed at symmetrical roles in relation to the Dolphin fish model's centerline and raised the fluid velocity flowing is apart from this model. The fluctuating velocity raise with the Dolphin fish model & NACA 0012 hydrofoil body. The thrust reach its maximum value at the tail end point.

The vortex shedding process initiates at the fish model shoulder, progressing through accumulation and growth along the fish's body before eventually detaching from the tail's end, fluctuating velocity attains a specific value. The front velocity is low when the fish was began, causing vortices closely positioned. Consequently, their effects synchronized, resulting in a substantial thrust force. However, model accelerated, vortices scattered, leading to a reduction in their overall effect. The considered cases are illustrated in Fig. 14, encompassing various propulsive Strouhal numbers for both models. These numbers determined for a combination of three different frequencies and three swimming velocities.

Both models' minimum Strouhal numbers are within their optimal propulsion regimes. There is a reasonable agreement of 98% achieved at a level of lower frequency and speed. The deviation is increased to around 5 %

while swimming at higher frequency and speed because of the turbulence effect of both the models.

6. CONCLUSION

In this work, a computational framework inspired by the pattern of swimming behavior of Dolphin fish was developed to facilitate the necessary adaptation in the starting fluctuating position its amplitude. As an agreement between both the models is reasonable, future researches can be completed in shorter computational time and cost by using NACA0012 hydrofoil instead of Dolphin-like fish model. The NACA0012 model has been shown to be an effective substitute simulation framework for replicating the underwater swimming technique. The proposed numerical model of both NACA0012 hydrofoil and Dolphin-fish framework with the finite volume method showed good agreement. Dolphin fish model was able to accomplish free swimming from the start to the exploring procedure. When its speed increases, the coefficient of drag decreases due to scenarios such as increased pressure at the Dolphin head, which generates high opposite force, its wake field is reducing in the vortices leading a low effect.

The pressure region ahead of the Dolphin model appeared larger during the cruising process. Consequently, it became imperative to diminish the fluctuating amplitude at the Dolphin's leading face in the kinematic model. This adjustment was crucial in reducing the opposite force and enhancing the overall fluid dynamic performance. This superposition of vortices helped for weakening the positive effect as proved in numerical simulation.

The minimum Strouhal numbers for both models align with their most efficient propulsion regime. Notably, a significant degree of concordance, approximately 98%, was attained when operating at lower frequencies and speeds. However, as the frequency and speed increased, reaching higher levels, a deviation of around 5% emerged due to the turbulence effects inherent to both models.

The effect of Strouhal number on vortex distribution was discussed. This research will serve as a valuable resource in the development of underwater robots and vehicles. In the future, there is potential for the creation of model with more joint to emulate the flexible model with motion. Furthermore, achieving a buoyancy control mechanism will be essential for experimental verification of the conclusions.

ACKNOWLEDGEMENTS

The authors would like to acknowledge all the persons who helped us in this work, in the computational fluid dynamics laboratory at PSG College of Technology in Coimbatore, India.

CONFLICT OF INTEREST

The authors declare that they have no competing interests.

AUTHORS CONTRIBUTION

T. Prabu: Methodology, Investigation, Supervision, Validation & Review. **A. Firthouse:** Writing, CFD analysis manuscript & editing. **A. M. Baranitharan:** Modelling, CFD analysis & Writing.

REFERENCES

- Anderson, J. M., Streitlien, K., Barrett, D. S., & Triantafyllou, M. S. (1998). Oscillating foils of high propulsive efficiency. *Journal of Fluid Mechanics*, 360, 41–72. <https://doi.org/10.1017/S0022112097008392>
- Borazjani, I., Sotiropoulos, F., Tytell, E. D., & Lauder, G. V. (2012). Hydrodynamics of the bluegill sunfish C-start escape response: three-dimensional simulations and comparison with experimental data, *The Journal of Experimental Biology*, 215(4), 671–684. <https://doi.org/10.1242/jeb.063016>
- Borazjani, I., & Sotiropoulos, F. (2008). Numerical investigation of the hydrodynamics of carangiform swimming in the transitional and inertial flow regimes. *The Journal of Experimental Biology*, 211, 1541–1558. <https://doi.org/10.1242/jeb.015644>
- Brücker, C., & Bleckmann, H. (2007). Vortex dynamics in the wake of a mechanical fish. *Experiments in Fluids*, 43, 799–810. <https://doi.org/10.1007/s00348-007-0359-2>
- Chen, H. W., Zhang, P. F., Zhang, L. W., Liu, H. L., Jiang, Y., Zhang, D. Y., & Jiang, L. (2016). Continuous directional water transport on the peristome surface of *Nepenthes alata*. *Nature*, 532, 85–89. <https://doi.org/10.1038/nature17189>
- Gen-Jin D., & Xi-Yun L. (2005). Numerical analysis on the propulsive performance and vortex shedding of fish-like traveling wavy plate, *International Journal for Numerical Methods in Fluid*, 48(12), 1351–1373. <https://doi.org/10.1002/flid.984>
- Guo, X. Q., Chen, D., & Liu, H. (2015). Does a revolving wing stall at low Reynolds numbers. *Journal of Biomechanical Science and Engineering*, 10, 1–10. <https://doi.org/10.1299/jbse.15-00588>
- Hemmati, A., Van Buren, T., & Smits, A. J. (2019). Effects of trailing edge shape on vortex formation by pitching pan-els of small aspect ratio. *Physical Review Fluids*, 033101(4), 1–27. <https://doi.org/10.1103/PhysRevFluids.4.033101>
- Jindong L., & Huosheng H. (2004). A 3D simulator for robotic fish, *International Journal of Automation and Computing*, 1(1), 42–50. <https://doi.org/10.1007/s11633-004-0042-5>
- Lauder, G. V. (2011). Swimming hydrodynamics: Ten questions and the technical approaches needed to resolve them. *Experiments in Fluids*, 51, 23–35. <https://doi.org/10.1007/s00348-009-0765-8>
- Leroyer, A., & Visonneau, M. (2005). Numerical methods for RANSE simulations of a self-propelled fish-like body, *Journal of Fluids and Structures*, 20 (7), 975–991. <https://doi.org/10.1016/j.jfluidstructs.2005.05.007>
- Li, N., Liu, H., & Su, Y. (2017). Numerical study on the hydrodynamics of thunniform bio-inspired swimming under self-propulsion. *PloS One*, 12(3), 1–36. <https://doi.org/10.1371/journal.pone.0174740>
- Mohammadshahi, D., Yousefi-Koma, & Bahmanya (2008, May 27-30). *Design, fabrication and hydrodynamic analysis of a biomemetic fish*. 10th WSEAS Int. Conf. on Automatic Control, Modelling & Simulation (ACMOS'08), Istanbul, Turkey. https://www.researchgate.net/publication/233379444_Design_Fabrication_and_Hydrodynamic_Analysis_of_a_Biomimetic_Robot_Fish
- Ou X., Aiguo S., Ji Y., Qixin Z. & Yong Y. (2020). Study on hydrodynamics of a flexible fishlike foil undulating in wall effect, *Engineering Applications of Computational Fluid Mechanics*, 14(1), 593–606. <https://doi.org/10.1080/19942060.2020.1745891>
- Ren, G., Dai, Y., Cao, Z., & Shen, F. (2015). Research on the implementation of average speed for a bionic robotic dolphin, *Robotics and Autonomous Systems*, 74, 184–194. <https://doi.org/10.1016/j.robot.2015.07.014>
- Strefling, P. C., Hellum, A. M., & Mukherjee, R. (2011). *Modeling, simulation, and performance of a synergistically propelled ichthyoids*. IEEE/RSJ International Conference on Intelligent Robots and Systems IEEE/ASME Trans. Mechatronics, 17(1), 36–45. San Francisco, CA, USA <https://ieeexplore.ieee.org/document/6094934>
- Triantafyllou, M. S., Triantafyllou, G. S. (2000). Hydrodynamics of fishlike swimming, *Annual Review of Fluid Mechanics*, 32, 33–53. <https://doi.org/10.1146/annurev.fluid.32.1.33>
- Wang, C., Tai, H., & Huang, H. R. (2015). Design and development of an autonomous underwater vehicle–robot dolphin, *Journal of Marine Engineering & Technology*, 14(1): 44–55. <https://doi.org/10.1080/20464177.2015.1022383>
- Wang, Z., Huang, B., Zhang, M., Wang, G., & Zhao, X. (2018). Experimental and numerical investigation of ventilated cavitating flow structures with special emphasis on vortex shedding dynamics. *International Journal of Multiphase Flow*, 98, 79–95. <https://doi.org/10.1016/j.ijmultiphaseflow.2017.08.014>
- Wen, L., Wang, T. M., Wu, G. H., & Liang, J. H. (2013). Quantitative thrust efficiency of a self-propulsive robotic fish: Experimental method and hydrodynamic investigation. *IEEE/ASME Transactions on Mechatronics*, 18, 1027–1038.

<https://doi.org/10.1109/TMECH.2012.2194719>

- Wu, Z., Yu, J., & Su, Z. (2015, September 6-9). *Design and CFD analysis for a biomimetic dolphin-like underwater glider*. Proceedings of International Conference on CLAWAR.
- Xue G., Liu Y., Si W., Xue Y., Guo F. & Li Z. (2020). Evolvement rule and hydrodynamic effect of fluid field around fish-like model from starting to cruising. *Engineering Applications of Computational Fluid Mechanics*, 14(1), 580-592. <https://doi.org/10.1080/19942060.2020.1734095>
- Zhang, Y. R., Kihara, H., & Abe, K. (2018). Three-dimensional simulation of a self-propelled fish-like body swimming in a channel. *Engineering Applications of Computational Fluid Mechanics*, 12(1), 473–492. <https://doi.org/10.1080/19942060.2018>.
- Zhou, H., Hu, T., & Low, K. H. (2015). Bio-inspired flow sensing and prediction for fish-like undulating locomotion: A CFD aided approach, *Journal of Bionic Engineering*, 12(3), 406–417. [https://doi.org/10.1016/S1672-6529\(14\)60132-3](https://doi.org/10.1016/S1672-6529(14)60132-3)